THE JOURNAL OF BIOLOGICAL CHEMISTRY VOL. 284, NO. 11, pp. 7165–7176, March 13, 2009

Interaction of APC/C-E3 Ligase with Swi6/HP1 and Clr4/Suv39 in Heterochromatin Assembly in Fission Yeast*[S]◆

Received for publication, August 20, 2008, and in revised form, December 22, 2008 Published, JBC Papers in Press, December 30, 2008, DOI 10.1074/jbc.M806461200

Rudra Narayan Dubey[1,2], **Nandni Nakwal**[1,3], **Kamlesh Kumar Bisht**[3], **Ashok Saini**[3], **Swati Haldar**[3], **and Jagmohan Singh**[4]

From the Institute of Microbial Technology, Sector 39A, Chandigarh-160036, India

Heterochromatin assembly in fission yeast is initiated by binding of Swi6/HP1 to the Lys-9-dimethylated H3 followed by spreading via cooperative recruitment of Swi6/HP1. Recruitment of Cohesin by Swi6/HP1 further stabilizes the heterochromatin structure and integrity. Subsequently, polyubiquitylation of Cut2 by anaphase-promoting complex-cyclosome (APC/C)-ubiquitin-protein isopeptide ligase (E3 ligase) followed by degradation of Cut2 releases Cut1, which cleaves the Rad21 subunit of Cohesin, facilitating sister chromatid separation during mitosis. Here, we demonstrate a surprising role of APC/C in assembly of heterochromatin and silencing at mating type, centromere, and ribosomal DNA loci. Coincidentally with the loss of silencing, recruitment of Swi6, H3-Lys-9-Me2, and Clr4 at *dg-dh* repeats at *cen1* and the *K* region of *mat* locus is abrogated in mutants *cut4*, *cut9*, and *nuc2*. Surprisingly, both Cut4 and Cut9 are also highly enriched at these regions in wild type and depleted in *swi6*Δ mutant. Cut4 and Cut9 interact directly with Swi6/HP1 and Clr4, whereas the mutant Cut4 does not, suggesting that a direct physical interaction of APC subunits Cut4 and Cut9 with Swi6 and Clr4 is instrumental in heterochromatin assembly. The silencing defect in APC mutants is causally related to ubiquitylation activity of APC-E3 ligase. Like *swi6* mutant, APC mutants are also defective in Cohesin recruitment and exhibit defects like lagging chromosomes, chromosome loss, and aberrant recombination in the *mat* region. In addition, APC mutants exhibit a bidirectional expression of *dh* repeats, suggesting a role in the RNA interference pathway. Thus, APC and heterochromatin proteins Swi6 and Clr4 play a mutually cooperative role in heterochromatin assembly, thereby ensuring chromosomal integrity, inheritance, and segregation during mitosis and meiosis.

Heterochromatin plays a central role in the structural integrity of chromosomes and their faithful segregation during mitosis. Studies in fission yeast have revealed the participation of various pathways in the assembly of heterochromatin at the centromere, mating type, telomere, and rDNA[5] loci. A functional characteristic of the heterochromatin structure is the repression of any reporter gene placed within these loci: a phenomenon known as transcriptional gene silencing. The initiation of heterochromatin assembly involves a selective removal of acetyl groups from the Lys residues at 9 and 14 positions in histone H3 followed by methylation at Lys-9 by the histone methyltransferase Clr4/Suv39, a modification specific for heterochromatin regions in *Schizosaccharomyces pombe* and higher eukaryotes (1, 2). The primary structural component of heterochromatin is the widely conserved chromodomain protein Swi6/HP1 (1), which binds to Lys-9-dimethylated histone H3 (H3-Lys-9-Me2) through its chromodomain. Subsequently, multimerization of Swi6 is thought to bring about the folding of chromatin into a transcriptionally inactive heterochromatin structure (2). Swi6 and Clr4 perform a mutually cooperative role in the spreading of heterochromatin (3, 4). In contrast, H3-Lys-4 dimethylation (H3-Lys-4-Me2) by Set1 in fission yeast and higher eukaryotes is generally associated with active, euchromatic regions (5).

Recent advances have revealed a role of the RNAi pathway in the assembly of heterochromatin. Disruption of *dcr1*, *ago1*, and *rdp1* leads to the loss of silencing, which is correlated with the lower level of H3-Lys-9-Me2 and Swi6 in the heterochromatin regions (6). Further work has shown that the RNAi pathway plays a role in the establishment of heterochromatin but not for its spreading (4). The binding of Swi6 is also regulated through phosphorylation by the Hsk1-Dfp1 complex (7); mutations in the Hsk1-Dfp1 kinase complex reduce the binding of Swi6 to heterochromatin, leading to the loss of silencing, increased chromosomal segregation defects, and chromosomal loss during mitosis (7).

The stability of heterochromatin is further enhanced by recruitment of Cohesin by Swi6/HP1 (8, 9); lack of Cohesin

* This work was supported by a grant from the Department of Science and Technology, New Delhi. The costs of publication of this article were defrayed in part by the payment of page charges. This article must therefore be hereby marked "*advertisement*" in accordance with 18 U.S.C. Section 1734 solely to indicate this fact.
◆ This article was selected as a Paper of the Week.
[S] The on-line version of this article (available at http://www.jbc.org) contains a supplemental table.
[1] These authors contributed equally to the work.
[2] Present Address: Dept. of Pharmacology, University of Medicine and Dentistry of New Jersey, Robert Wood Johnson Medical School, Piscataway, NJ 08854.
[3] Supported by the Council for Scientific and Industrial Research senior research fellowships.
[4] To whom correspondence should be addressed. Tel.: 91-172-2636680, Ext. 3228; Fax: 91-172-2690585, 2690632; E-mail: jag@imtech.res.in.

[5] The abbreviations used are: rDNA, ribosomal DNA; APC/C, anaphase-promoting complex-cyclosome; E3, ubiquitin-protein isopeptide ligase; Ub, ubiquitin; Swi, switching; Clr, cryptic loci regulator; HP1, heterochromatin protein 1; RE, repression element; DAPI, 4,6-diamidino-2-phenylindole; Sng, silencing not governed; Cut, chromosomes untimely torn; Cdc, cell division control; DSB, double strand break; pol, polymerase; RNAi, RNA interference; HA, hemagglutinin; ts, temperature-sensitive; FOA, fluoroorotic acid; PMA, phorbol 12-myristate 13-acetate; IP, immunoprecipitation; ChIP, chromatin IP; Ni-NTA, nickel-nitrilotriacetic acid; RT-PCR, reverse transcription-PCR; WT, wild type; YE, yeast extract.

recruitment in *swi6*$^-$ mutant leads to chromosomal rearrangements in the mating type region and enhanced chromosomal loss (9). Cohesin is an evolutionarily conserved complex, comprising subunits Psm1, Psm3, Psc3, and Rad21 in fission yeast, which ensures sister chromatid cohesion at the centromeric loci as well as along the arm regions (8–10). During DNA replication, the sister chromatids are encircled by the Cohesin complex, which holds the sister chromatids together until late mitosis (11). During metaphase to anaphase transition, the Rad21 subunit of Cohesin is degraded to facilitate sister chromatid separation. This chain of molecular events is facilitated by the anaphase-promoting complex-cyclosome, APC/C-E3 ligase, which promotes polyubiquitination of Cdc13 and Cut2. Degradation of polyubiquitylated Cut2 by proteasome releases Cut1, which, in turn, degrades the Cohesin subunit Rad21 at the centromeric regions, ensuring sister chromatid separation during metaphase-to-anaphase transition (10, 12). Degradation of polyubiquitylated Cdc13 triggers the exit of the cells from mitosis.

Thus, APC is known to play an important role in sister chromatid separation and mitotic exit. On the other hand, Cohesin is thought to be recruited during DNA replication (11). Other results suggest that Swi6 may also be recruited during DNA replication (13, 14). In this context, the present study shows a novel role of APC/C in the assembly of heterochromatin. Mutations in APC subunits *cut4* and *cut9* abrogate gene silencing accompanied by reduced localization of Swi6, H3-Lys-9-Me2, and Clr4 to heterochromatin loci. Like *swi6*$^-$ and cohesin mutants, APC mutants also exhibit enhanced chromosomal loss, chromosomal rearrangements, and chromosomal segregation defects during mitosis and meiosis. Surprisingly, the APC subunits Cut4 and Cut9 are enriched at the heterochromatin regions, and this localization is dependent on Swi6. A direct physical interaction of Cut4 and Cut9 with Swi6 and Clr4 plays an important role in heterochromatin assembly, and the silencing and other defects of APC mutants may be ascribed to the inability of the mutant proteins to bind and recruit Swi6 and Clr4. Thus, APC/C and Swi6 and possibly Clr4 function together to ensure a cooperative recruitment of Clr4 and Swi6, leading to assembly of heterochromatin and thereby ensuring chromosomal integrity and segregation during mitosis and meiosis.

EXPERIMENTAL PROCEDURES

Strains and Plasmids—The following parental strains were used in most experiments. SP1152 (genotype: *Msmto REIIΔmat2*::*ura4 ura4D18 leu1-32, ade6-210*) and PG1649 (genotype: *mat1PΔ17*::*LEU2 REIIIΔmat3MEcoRV*::*ade6*, *leu1-32, ura4D18, ade6-210*) were used to monitor mating type silencing. For monitoring centromeric silencing, strain FY2002 was used (genotype: *h*$^+$ *leu1-32 ura4DS/E ade6DN/N imr1L*::*ura4 otr1R*::*ade6*). Strain HU393 was used to monitor silencing at rDNA locus (genotype: *h*$^+$ *leu1/YIP2.pUCura4*$^+$*/ura4-DS/E leu1-32 ade6-216*). Mutations were transferred into the above reporter strains by standard genetic crosses. The strains and plasmids used in this study are listed in supplemental Table 1. Media and growth conditions were as described (15). Chromosomal loss rates were determined by using a strain with *ade6-210* mutation and carrying an artificial chromosome *Ch-16* that contains *ade6-216* allele (16). In principle, this strain behaves as a wild type strain for *ade6* marker and produces white colonies on adenine-limiting plates (YE (15)) because of interallelic complementation. Mutations that cause chromosomal instability lead to the loss of *Ch-16*, forming colonies that produce pink pigmentation because of the remaining *ade6-210* allele (16). Chromosomal loss rates were determined according to Kipling and Kearsey (17). The rate of switching of the dark- and light-staining colonies was determined by growing cells from each colony for 20 generations, and the dark- and light-staining colonies before and after culturing for 20 generations were counted. The rate of switching was determined according to Kipling and Kearsey (17).

Strain and Plasmid Constructions—Strain carrying *swi6* deletion was constructed as described (18), whereas strain carrying deletion of *clr4* gene was constructed by PCR based disruption using the *kan*^{r} marker-based modules (19). Construction of His_6-tagged *clr4* gene was carried out in the vector pQE30 (Qiagen). Sequences of the primers can be supplied on request. To express HA-tagged Cut4, *cut4-533* mutant was transformed with the vector pREP41-N-HA-*cut4* (a gift from M. Yanagida), which complemented the silencing defect of the *cut4* mutant. The strain was grown using the regime for induction of *nmt* promoter (15). The strain expressing *sng2-1* mutant protein with HA tag was derived as leu$^-$ progeny by loop-out recombination from the stable Leu$^+$ transformants. These derivatives were checked for expression of HA-tagged Cut4 protein and temperature sensitivity to confirm that they expressed the mutant protein. Glutathione *S*-transferase-tagged Swi6 was expressed in the vector pGEX-2T, and the purified glutathione *S*-transferase-tagged Swi6 protein was injected subcutaneously into rabbits to raise anti-Swi6 antibody. The specificity of the antibody was confirmed by Western blotting.

Confocal and Immunofluorescence Microscopy—For microscopic examination, vegetative cells were stained with DAPI and anti-α-tubulin antibody followed by anti-mouse-fluorescein isothiocyanate antibody. Zygotic asci of sporulating cultures were stained with DAPI (15). Samples were examined under a Carl Zeiss LSM510 Meta confocal microscope.

Plate Assay for Silencing—Expression of the *ura4* reporter inserted at various loci in wild type and mutants was monitored by spotting 5-μl aliquots of 10-fold serial dilutions of cultures of the strains on complete plates, plates lacking uracil, and plates containing FOA. Plates were incubated at 25 °C for 4–5 days. Expression of the *ade6* reporter was monitored by streaking the cultures on YE plates and incubating at 25 °C for 4–5 days, and *cut9-665* mutant was also grown at 30 °C. Although the parent strains having the *ade6* locus in the repressed state at the *mat* or centromere loci produce red colonies, the mutant strains yield white or pink colonies. For checking silencing in the silencer deletion background, strains were also streaked on sporulation plates (PMA$^+$ (15)). After growth at 25 °C for 4–5 days, either colonies were stained with iodine or their cells were examined microscopically.

Chromatin Immunoprecipitation (ChIP) Assay—ChIP assay was performed as described earlier (20). The oligonucleotides

used were: ura4F, 5′-gaggggatgaaaaatcccat-3′; ura4R, 5′-ttcgacaacaggattacgacc-3′; ade6F, 5′-tgcgatgcacctgaccaggaaagt-3′; ade6R, 5′-agagttgggtgttgatttcgctga-3′; act1F, 5′-tcctacgttggtgatgaagc-3′; act1R, 5′-tccgatagtgataacttgac-3′; dhFor, 5′-ggagttgcgcaaacgaagtt-3′; dhRev, 5′-ctcactcaagtccaatcgca-3′; dhkFor, 5′-tatccaagtggaatgaacatgat-3′; dhkRev, 5′-tcgtttgaaacgatgaaatgga-3′. Cycling conditions were: 95 °C, 2 min; 30 cycles of 95 °C, 1 min; 55 °C, 30 s; 72 °C, 2 min; 72 °C, 10 min. PCR reactions included 0.1 μl of [α-^{32}P]dCTP (10 mCi/ml), and the products were resolved by polyacrylamide gel electrophoresis followed by autoradiography. Untagged strains, used as control, gave no signal in the IP reactions. Quantitation of the bands was done by densitometric analysis or on phosphorimaging device (Bio-Rad model Molecular Imager FX). Enrichment of Swi6 and histone modifications was quantitated by calculating the ratios of *dh*/*act1* or *dh-k*/*act1* signal for the IP sample *versus* whole cell extract control.

Co-immunoprecipitation and Pull-down Assays—Antibodies against HA or Swi6 were prebound at 1:50 dilution to 20 μl of IgG-Sepharose beads at 4 °C for 3 h on a tube rotator. In some cases, antibody was covalently cross-linked to the beads. Beads were then incubated overnight with 2–5 mg of the protein extract prepared from strains carrying HA-tagged *cut4* or *cut9* genes. All incubations were carried out in the presence of ethidium bromide (final concentration 50 μg/ml) to rule out DNA-dependent protein-protein interactions (21). Beads were washed 3–4 times with HB buffer (0.02 M HEPES, 0.1 M NaCl, 2 mM EDTA, 0.625% glycerol, 1 mM β-mercaptoethanol) and mixed with 1× SDS sample buffer. Samples were boiled for 5–10 min and subjected to SDS-PAGE followed by Western blotting with anti-HA antibody (1:1000) or anti-Swi6 antibody (1:10,000).

For pull-down assays, extracts were prepared from *Escherichia coli* strains expressing His_6-tagged Clr4 and allowed to bind to Ni-NTA resin (Qiagen (binding capacity 5–10 mg of protein/ml resin)), which was equilibrated with binding buffer (50 mM NaH_2PO_4, pH 8.0, 300 mM NaCl, 10 mM imidazole). Binding was carried out overnight at 4 °C. 3–4 washings were performed with binding buffer at 4 °C, and the beads were collected by centrifugation at 500 × *g* for 5 min. Crude extracts prepared from strains expressing HA-Cut4 and HA-Cut9 were then added to the above resin at increasing concentrations from 100 to 600 μg along with control, 1 mg/ml bovine serum albumin, and 1× binding buffer (5× binding buffer (750 mM NaCl, 100 mM Tris-Cl, pH 8.0, 5 mM EDTA, 5 mM dithiothreitol)). Samples were incubated at 4 °C for 3–4 h to overnight and then washed four times with washing buffer (same as HB buffer. To the above samples, 1× SDS loading buffer was added. Samples were boiled for 5–10 min, subjected to SDS-PAGE, Western blotted, and probed with anti-HA antibody. Domain interactions were studied in a similar manner.

RT-PCR, Northern, and Western Blotting—Preparation of RNA followed by Northern blotting and hybridizations as well as RT-PCR were performed as described earlier (13). Western blotting was performed by using the semidry blotter as per the manufacturer's instructions (Sigma). After transfer, the membrane was blocked overnight with 5% skim milk in 1× phosphate-buffered saline at 4 °C. The membrane was incubated with the primary antibody at 1:1000 dilution for anti-HA antibody and 1:10,000 dilution in the case of anti-Swi6 antibody. Anti-mouse AP-conjugated secondary antibody was used at 1:20,000 dilution. Alternatively, horseradish peroxidase-conjugated secondary antibody was used at the same dilution followed by detection using the ECL kit (Millipore). Incubations with antibodies and substrates were performed as per the manufacturer's instructions (Santa Cruz Biotechnology, Sigma, Millipore).

RESULTS

Role of APC Subunits in Silencing of Mating Type, Centromere, and rDNA Loci—This study began from a screen designed to isolate mutants in essential genes that may act in the same pathway of silencing as *swi6*, *clr1–clr4*. We screened for temperature-sensitive (ts) mutants in a strain harboring a stable *mat1M* locus (*Msmto*) and *mat2* locus having its silencer *REII* deleted and carrying a *ura4* reporter insertion (genotype: *mat1Msmto REII*Δ *mat2*::*ura4*). The ts mutants were screened for the formation of colonies that gave dark staining with iodine and displayed haploid meiosis upon microscopic examination (these phenotypes are associated with the loss of silencing (15)). After screening for about 50,000 colonies, 10 colonies were isolated that both exhibited a temperature-sensitive phenotype (they grew well at 25 °C but did not grow at 36 °C upon replica plating) and gave dark staining with iodine, indicative of silencing defect. One out of these silencing defective mutants gave a very strong ts phenotype at 36 °C. It was named as *sng2-1* (silencing not governed 2-1) and studied further.

The mutant *sng2-1* exhibited two alternate states of silencing. One, named Light (*L*), produced colonies, most of which gave no staining with iodine and lacked haploid meiosis when grown on minimal medium. The other, named Dark (*D*), produced colonies, most of which gave dark staining with iodine staining and whose cells showed haploid meiosis phenotype. These states were metastable, switched at a low rate ($\sim 10^{-4}$/generation) among each other (Fig. 1*A*), and may represent alternative heritable chromatin states that are stably inherited during mitosis, as described earlier (22, 23). RT-PCR analysis of cells from dark-staining colonies showed high level of expression of the *ura4* reporter gene as compared with the cells from light-staining colonies (Fig. 1*D*). Results of a plate assay confirmed the above results (Fig. 1*B*). Genetic studies led to the identification of the gene encoding the *sng2-1* locus as *cut4*, which encodes the largest subunit of APC/C (12)).

To address the obvious question whether the other subunits of APC are also involved in silencing, the effect of mutations in Cut4 and Cut9 subunits of APC on silencing was tested next. Like *sng2-1*, *cut4-533*, and *cut9-665* mutants also showed loss of silencing in the strain background *mat1Msmto REII*Δ*mat2*::*ura4*, as indicated by dark staining of colonies with iodine (Fig. 1*C*) and expression of the *ura4* reporter by RT-PCR (Fig. 1*D*). Further, like *sng2-1*, *cut4-533* and *cut9-665* mutants also exhibited dark- and light-staining colonies (Fig. 1*C*). Although the dark colonies had a higher level of *ura4*, the light colonies showed much lower expression of *ura4* transcript (Fig. 1*D*), which correlated with the level of the growth of cells on plates lacking uracil and lack of growth on plates containing

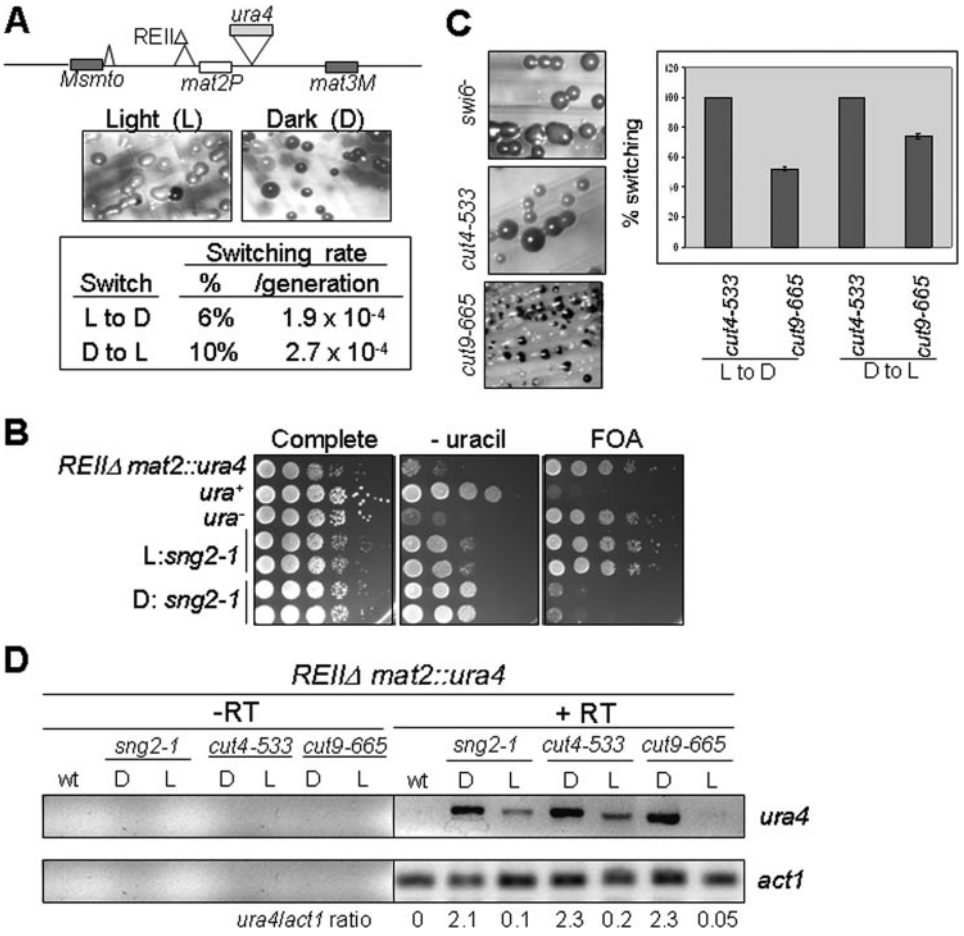

FIGURE 1. ***sng2-1/cut4⁻, cut4-533, and cut9-665* mutant exhibit two alternative states of expression of silent *mat2* locus.** *A*, *sng2-1* mutant having the *mat2*-proximal silencer deleted (*REIIΔ*) exhibits light (*L*) and dark (*D*) colonies upon iodine staining, which are metastable and switch to the opposite state at a low rate. The rate of switching was determined according to Ref. 17. *B,* the light and dark states show low and high levels, respectively, of *ura4* expression as monitored by serial dilution assay on plates lacking uracil or containing FOA. *C*, *cut4-533* and *cut9-665* mutants also exhibit the two epigenetic states of silencing in the strain background *Msmto REIIΔ mat2::ura4*, which show relatively less stability than the *sng2-1* mutant histogram. *D*, the dark (*D*) and light (*L*) colonies exhibit high and low levels of *ura4* transcripts, respectively. RT-PCR for *ura4* and *act1* as a negative control was carried out according to Singh *et al.* (41).

FOA. Thus, APC plays a role in stable repression of the *mat2P* locus. In addition, like *sng2-1*, both *cut4-533* and *cut9-665* mutations also abrogated silencing of the *ade6* reporter gene inserted at *mat3* locus, with the flanking cis-acting repression element, *REIII*, deleted (genotype: *REIIIΔ mat3::ade6*); the loss of silencing was indicated by the growth of pink and white colonies on adenine-limiting medium as well as dark iodine staining on sporulation plates (PMA^+ (15)). Similar phenotype has been shown to be displayed by *swi6* and *clr1-clr4* mutants (24). These findings encouraged us to think that *cut4* and *cut9* may act in the same pathway as *swi6*.

To check whether APC is involved in silencing at other heterochromatin regions, we studied the effect of APC mutations on silencing at the centromere loci. *sng2-1*, as well as *cut4* and *cut9* mutations, caused derepression of *ade6* reporter at *otr1R* repeat of *cen1*, as indicated by the appearance of pink and white colonies on adenine-limiting plates (Fig. 2*B*). However, none of these mutations were found to affect expression of *ura4* reporter placed at *cnt1* and *imr1R* regions of *cen1* (data not shown). Similarly, the *Saccharomyces cerevisiae LEU2* and/or *S. pombe ura4* reporter genes inserted at rDNA loci were derepressed in all three mutants (although strongly in the case of *cut4-533* and only modestly in *sng2-1/cut4⁻* and *cut9-665* mutants), as indicated by growth on plates lacking leucine or uracil and lack of growth on FOA plates (Fig. 2*C*). However, none of these mutations affected telomere silencing (data not shown).

Mutations in APC Subunits Abrogate the Localization of Swi6/HP1 and H3-Lys-9-Me2 at Mating Type and cen Loci—Cut4, along with Cut9, Nuc2, and other proteins, forms an active anaphase-promoting complex, which functions as an E3 ubiquitin ligase (12, 25). The major protein targets of APC play a role during mitotic exit (Cdc13) and metaphase-to-anaphase transition (Cut2 (10, 12)). Degradation of Cut2 following APC-mediated polyubiquitylation releases Cut1, which degrades the Rad21 subunit of Cohesin during the metaphase-to-anaphase transition. Swi6, which is implicated in silencing, has been shown to recruit Cohesin, possibly during replication (11), leading to further stabilization of the chromatin organization (8, 9). Thus, it is surprising to note that APC/C-E3 ligase, whose time of function involving Cut2 and Cdc13 degradation occurs during mitosis (26), could also be involved in silencing. Nonetheless, we checked the localization of Swi6 and H3-Lys-9-Me2, which are known to be associated with heterochromatin (2), at the *otr1R* repeat of *cen1* and silent mating type locus. Because of the fact that *dh* repeats at *cen1* and similar sequences located within the *mat2-mat3* interval (27) comprise the putative sites of initiation of heterochromatin (4), together with our finding that, like RNAi mutants, APC mutants also show bidirectional transcription from *dh* repeats (see below), we chose to quantitate the enrichment of H3-Lys-9-Me2 and Swi6 at these sites. Results of ChIP analysis (20) showed that the localization of both Swi6 and H3-Lys-9-Me2 at the *dh* repeat at *otr1R* (Fig. 3, *A* and *B*) as well as *dh-k* repeat in the *K* region (*cenH*) spanning the *mat2-mat3* interval (Fig. 3, *C* and *D*) was drastically reduced in *sng2-1*, *cut4-533*, and *cut9-665* and *nuc2* mutants. Surprisingly, the level of H3-Lys-9-Me2 was also reduced in *swi6Δ* strain at both *otr1R* and *cenH* (Fig. 3). Although some studies have shown no change in the level of H3-Lys-9-Me2 in *swi6Δ* mutant (28), Kim *et al.* (29) did show a reduced level of H3-Lys-9-Me2 in *swi6Δ* mutant. Similarly, Hall *et al.* (4) showed that, whereas the site of

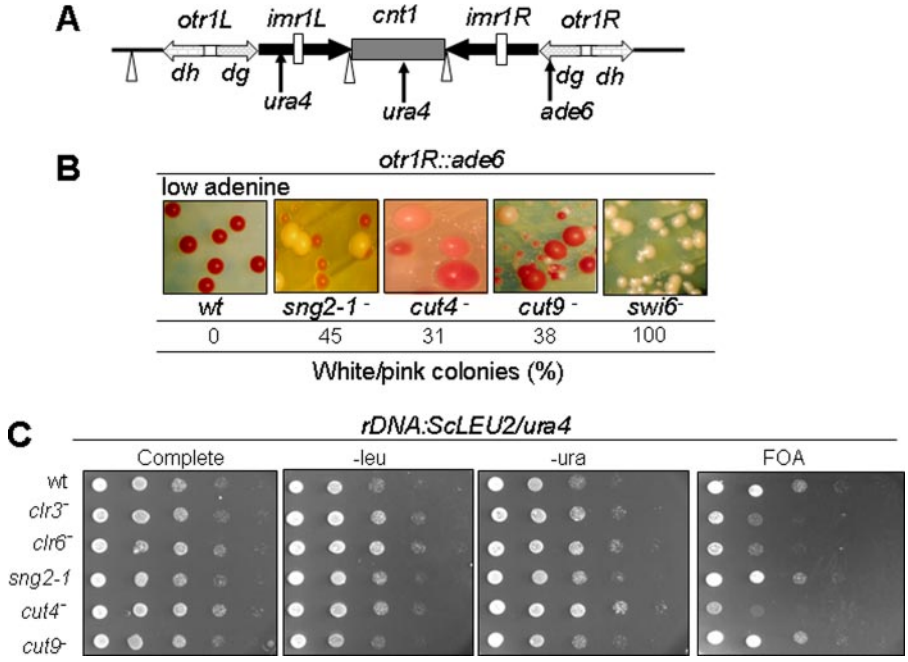

FIGURE 2. **Effect of mutations in APC subunits on silencing at centromere and rDNA loci.** *A*, schematic organization of *cen1* locus, indicating the *cnt1*, inner repeats *imr1L* and *imr1R*, and outer repeats *otr1L* and *otr1R* and showing the insertion of *ura4* reporter at *cnt1* and *imr1L* and *ade6* at *otr1R*. Sites of location of the single and clustered tRNA genes are indicated by *inverted triangle* and *vertical bars*, respectively. *B*, silencing defect at the outer repeat region in APC mutants. Strains harboring *ade6* reporter at *otr1R* region of *cen1* in WT, *sng2-1*, *cut4-533, cut9-665*, and *swi6*Δ mutant backgrounds were streaked on YE (adenine-limiting (15)) plates and allowed to grow at 25 °C for 4–5 days, and *cut9-665* mutant was streaked at 30 °C. The number of white or pink colonies, representing the derepressed state of *ade6* reporter, as a percentage of total colonies, was counted. *C*, the loss of silencing of reporters inserted at rDNA loci in APC mutants. Wild type strain and strains of *sng2-1*, *cut4*, *cut9*, *clr3*, and *clr6* mutants in the genetic background where *LEU2* gene of *S. cerevisiae* and *ura4* gene of *S. pombe* are inserted at the rDNA locus were grown, and 10-fold serial dilutions were spotted on complete plates and plates lacking leucine or uracil and plates containing FOA. The plates were allowed to grow at 25 °C for 4–5 days and photographed.

nucleation of heterochromatin at the *cenH* region shows less effect of *swi6*Δ mutation on the level of H3-Lys-9-Me2, the flanking regions do show a drastic decrease. These results suggested a role of Swi6 in spreading the H3-Lys-9 methylation (4), which possibly involves interaction between Swi6 and Clr4.

Although the effect of *nuc2* mutation on silencing could not be checked directly because the sterility of *nuc2* mutant strains prevented construction of the necessary strains (30), *nuc2* mutant also showed a reduced localization of both Swi6 and H3-Lys-9-Me2 at the *dh* and *dh-k* regions (Fig. 3). Thus, Nuc2 is also involved in silencing by regulating the localization of Swi6 and H3-Lys-9-Me2 at the mating type and outer repeat *otr1R* of *cen1* locus.

Because there is a reciprocal relationship between the localization of H3-Lys-9-Me2 and H3-Lys-4-Me2, with the former being elevated and the latter depleted in the heterochromatin domains in *S. pombe* (5), we also quantitated the level of H3-Lys-4-Me2. Interestingly, the level of H3-Lys-4-Me2 was elevated at the *otr1R* repeat in *cut4-533* mutant as well as *sng2-1* and *cut9* mutants (data not shown). Further, the distribution pattern of green fluorescent protein-tagged Swi6, which is localized predominantly at three foci in a large percentage of interphase cells in the wild type (31), is drastically altered in *sng2-1, cut4-533*, and *cut9-665* mutants, with a preponderance of cells having one or two foci. Thus, *sng2-1*, *cut4-533*, and *cut9-665* (and possibly *nuc2*) mutations reduce the level of H3-Lys-9-Me2 and Swi6 and may exert similar effect at the *dh-k* repeats in the *mat2-mat3* interval.

Because Clr4 performs histone H3-Lys-9 dimethylation and Swi6 binds to H3-Lys-9-Me2, we next checked whether APC subunits are required for recruitment of Clr4 as well. Results showed that Clr4 is enriched at the *dh* region of *cen1* in wild type strain but is delocalized in the *cut4-533* mutant. Thus, the reduction in the level of H3-Lys-9-Me2 in *cut4*, *cut9*, and *nuc2* mutants may result from reduced localization of Clr4 to heterochromatin. We think that a lack of interaction between the mutant Cut4 protein and Clr4 may be responsible for this defect (see below).

Recruitment of Cut4p and Cut9p to Heterochromatin Is Swi6-dependent—We also checked the converse possibility: whether Cut4p and Cut9p are localized to heterochromatin and, if so, whether this localization is dependent on Swi6. ChIP analysis was carried out using strains in which *cut4* and *cut9* genes were tagged with the HA epitope. HA tagging had no adverse effect on the growth rate of cells and silencing (data not shown). Surprisingly, the results showed that both Cut4 and Cut9 are highly enriched at the *dh* sequences in *otr1R* and *dh-k* repeats in the *cenH* region spanning the *mat2-mat3* interval (Fig. 4, *A*–*C*). Control blots using untagged strains showed no signal in the IP reactions (not shown). Remarkably, the localization of Cut4p and Cut9p at both the regions was almost completely abolished in *swi6*Δ strain (Fig. 4, *A*–*C*). Thus, surprisingly, not only is the APC localized to heterochromatin, its localization is also dependent on Swi6. Taken together, the above results suggest that Swi6 and APC may cooperate to bring about mutual recruitment and establishment of heterochromatin.

Cut4 and Cut9 Interact with Swi6/HP1 and Clr4—The above results suggested the possibility of direct interaction between APC subunits and heterochromatin proteins Swi6 and Clr4. Interestingly, both HA-tagged Cut4 and HA-tagged Cut9 could be specifically co-immunoprecipitated with anti-Swi6 antibody (Fig. 5*A*). This interaction was observed in the presence of EtBr (Fig. 5*A*), ruling out the possibility that Cut4 and Cut9 interacted with Swi6 indirectly through DNA. A reciprocal co-immunoprecipitation experiment showed that Swi6 could also be immunoprecipitated with Cut4 and Cut9 using anti-HA antibody in strains expressing HA-tagged Cut4 and Cut9 (Fig. 5*A*, *bottom panel*). In pull-down experiments, both HA-tagged Cut4 and HA-tagged Cut9 could be specifically bound to Ni-NTA resin on which His_6-tagged Clr4 was immobilized (Fig.

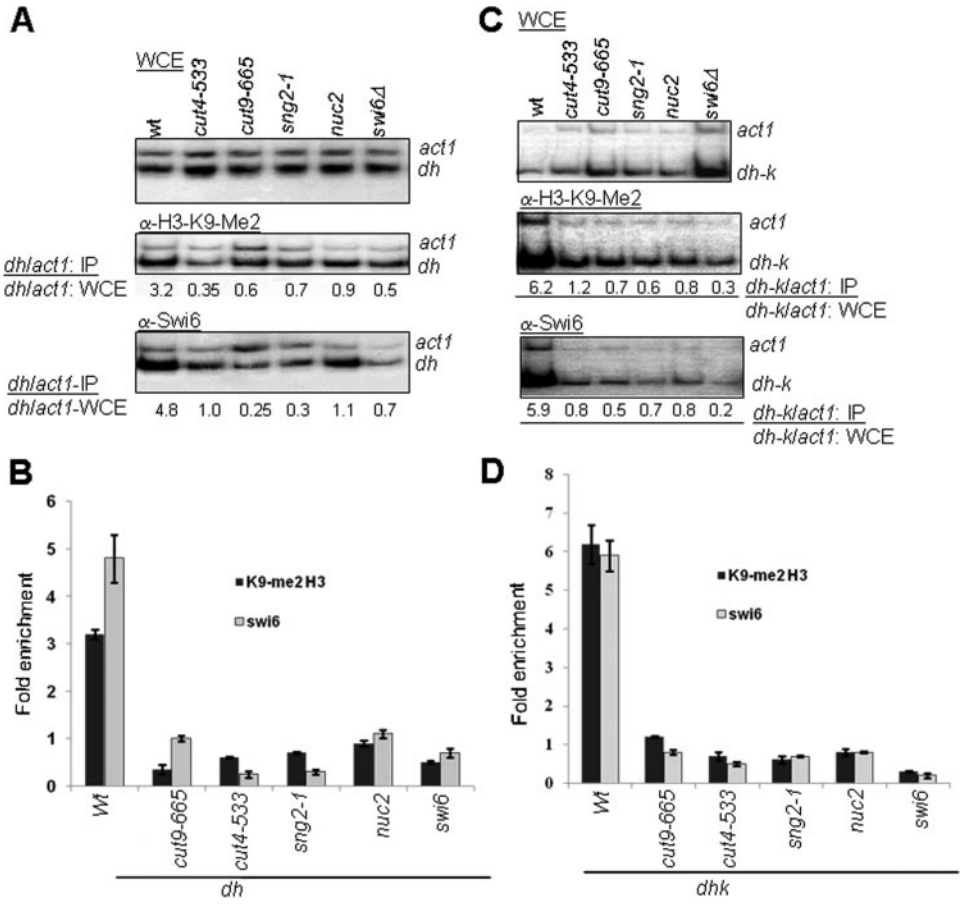

FIGURE 3. **Role of APC in recruitment of Swi6 and H3-Lys-9-Me2 to heterochromatin regions.** APC subunits Cut4, Cut9, and Nuc2 are required for recruitment of Swi6 and establishing the H3-Lys-9-Me2 mark at the mating type and centromeric regions. *A–D*, reduced localization of Swi6 and M3-Lys-9-Me2 at the *dh* region of the *otr1R* repeat of *cen1* (*A* and *B*) and at the *dh-k* repeat in the *K* region spanning the *mat2-mat3* interval in *sng2-1/cut4*$^{-}$, *cut4-533, cut9-665*, and *nuc2* mutants (*C* and *D*). *swi6*Δ strain was used as a positive control. Cultures of most strains were grown at 25 °C, except *cut9-665*, which was grown at 30 °C. ChIP experiments were performed using rabbit polyclonal antibody against Swi6 and monoclonal antibody against H3-Lys-9-Me2 (Upstate Biotechnology). The enrichment ratio was quantitated from yields of PCR products representing the *dh* and *dh-k* sequences amplified under logarithmic stage of amplification, using *act1* as a negative control. *B* and *D* show the histograms representing the average of three independent experiments. *WCE*, whole cell extract.

5*B*). Similar experiments with the mutant *sng2-1*/*cut4*$^{-}$ tagged with HA epitope showed a lack of interaction of the mutant protein with Swi6, as shown by co-immunoprecipitation (Fig. 5*C*, *top panel*), and with Clr4, as shown by pull-down assay (Fig. 5*C*, *bottom panel*). A pull-down experiment of HA-tagged Cut9 with His_6-tagged RibC protein from *Bacillus* sp. failed to show any interaction (Fig. 5*D*, *left panel*). Similarly, HA-tagged Rad21 protein showed no interaction with His_6-Clr4 in a pull-down assay (Fig. 5*D*, *right panel*). Taken together, these results support the inference that APC plays a role in heterochromatin assembly by recruitment of both Clr4 and Swi6 by direct physical interaction through its subunits Cut4 and Cut9 and that the silencing defect in *sng2-1* mutant can be correlated with the loss of binding of the mutant Sng2-1/Cu4 protein with Swi6 and Clr4.

Interaction of Cut4 and Cut9 with the domains of Clr4 was checked by *in vitro* pull-down experiments. Results showed that although Cut9 interacted relatively weakly with chromodomain (CD) and pre-SET (suppressor of variegation-enhancer of zeste-trithorax) domains of Clr4, Cut4 interacted more strongly with both the domains, with a greater binding to the chromodomain (data not shown).

Defects in Centromeric Cohesin Recruitment and Chromosome Dynamics during Mitosis and Meiosis in APC Mutants—Because reduced Swi6 localization affects recruitment of Cohesin, we checked the effect of mutations in APC subunits, which are shown above to reduce the heterochromatic localization of Swi6, on cohesin recruitment to *dh* repeats in the *otr1R* region of *cen1*. Results showed a reduction in the localization of Rad21 at the *dh* sequences of *otr1R* region by 3–5-fold in the *sng2-1*, *cut4-533*, and *cut9-665* mutants. A slightly reversed effect was observed at the arm regions, like *ura4* or *cdc25*, which may occur due to redistribution of Rad21/cohesion complex. Thus, APC plays a surprising new role in the assembly of centromeric heterochromatin, which, in turn, recruits Cohesin at centromeres.

Because earlier studies showed that the loss of Cohesin in *swi6* mutant leads to reduced chromosomal integrity, we checked the effect of mutations in APC subunits. Indeed, *sng2-1*, *cut4-533*, and *cut9-665* mutants also exhibit increased rates of chromosomal loss, as monitored by the loss of the artificial Ch16 chromosome (Fig. 6*A*). Microscopic analysis of mitotic cells was carried out to investigate the chromosomal segregation defects also reported earlier in *swi6* and cohesin mutants (9, 32). Results showed enhanced fraction of cells with aberrant chromosomal segregation phenotypes, like lagging chromosomes, in *sng2-1*, *cut4-533*, and *cut9-665* mutants (Fig. 6*B*), similar to the phenotypes of *swi6*, *rik1*, and *clr4* mutants (33). To further check the nature of mitotic phenotypes, we carried out microscopic examination after staining the nuclei and cell septa simultaneously. Results showed a higher incidence of defective nuclear segregation and septum formation without cell separation and lack of nuclei in daughter cells in *sng2-1*, *cut4-533*, and *cut9-665* mutants (data not shown).

Because both *swi6* and cohesin mutants have been shown to exhibit an enhanced rate of aberrant recombination in the mating type region (9), we analyzed the homothallic, switching (h^{90}) strains of *sng2-1*, *cut4-533*, and *cut9-665* mutants. (The homothallic strains are the efficiently switching strains that contain the native mating type configuration comprising the

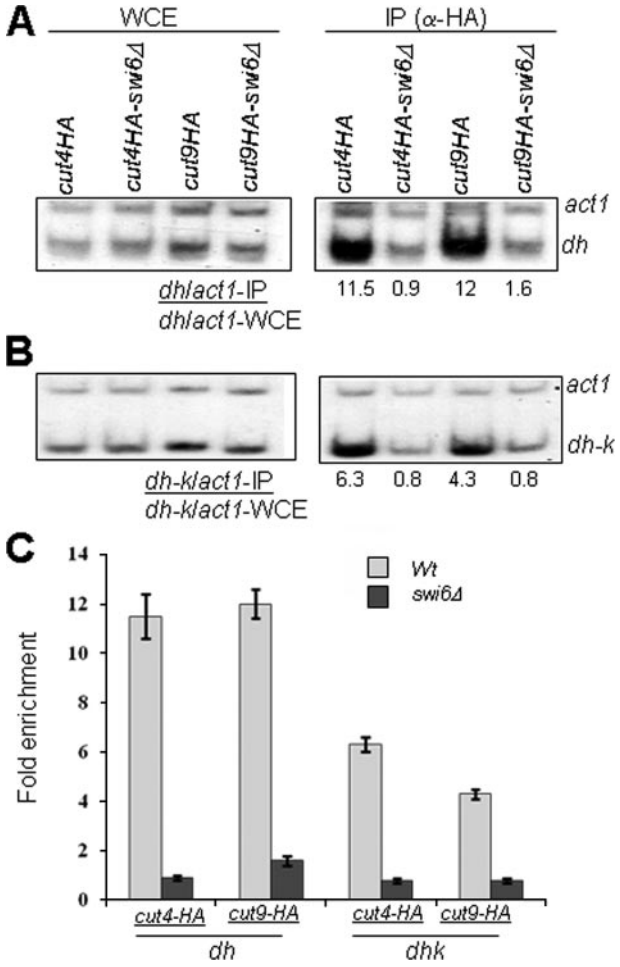

FIGURE 4. **Cut4 and Cut9 are localized at *cen* and *mat* regions in a Swi6-dependent manner.** *A* and *B*, localization of Cut4 and Cut9 at the *dh* region of *cen1* (*A*) and at *dh-k* region in the *mat2-mat3* interval (*B*) is abrogated in *swi6*Δ mutant. Localization of Cut4 and Cut9, which were tagged with HA epitope, was quantitated in WT and *swi6*Δ mutant background by ChIP assay, using *act1* as a negative control. Each experiment was done thrice. *WCE*, whole cell extract. *C* shows the quantitation of the averaged data.

mat1P/M, *mat2P*, and *mat3M* loci with HindIII fragment sizes of 10.4, 6.3, and 4.2 kb, respectively, as detected by Southern blot hybridization. Because of efficient switching, such strains have a roughly equal number of cells of Plus and Minus mating type, which mate and sporulate; the spores of the resulting asci contain a starchy compound that gives dark staining with iodine (15). Thus, dark staining of a homothallic strain is indicative of intactness of the mating type configuration, as mentioned above.) Interestingly, all the mutants generated derivatives with low iodine staining, a phenotype associated with reduced mating type switching (34, 35) (Fig. 6*C*). A reduction in the rate of switching and iodine staining has been associated either with a reduced level of the double-strand break (DSB) at the switching recipient *mat1* locus or with lower efficiency of switching or with rearrangements in the mating type organization, like h^+, which results from duplication of *mat2-mat3* interval on to the *mat1* locus (34, 35). Interestingly, both *cut4-533* and *cut9-665* mutants generated derivatives lacking the DSB (Fig. 6, *C* and *D*, *lanes 2*, *3*, and *7*; see the figure legend) as well as rearrangements in the mating type region (Fig. 6, *C* and *D*, *lanes 4* and *6*), although the rearrangements are somewhat different from those reported earlier (9, 34). Thus, as in the case of *swi6* and cohesin mutants, the integrity of mating type region was also abrogated in derivatives of APC mutants. The effect on DSB is surprising because *swi6* mutant also frequently generates h^+ rearrangements but does not produce derivatives without DSB (9, 34). It is possible that the effect on DSB may be due to the possible interaction of Cut4 with DNA polα, as suggested by the fact that *polα* can suppress the ts phenotype of *sng2-1* and *cut4-533* mutants and polα, in turn, is known to be involved in generating the DSB (36).

It is pertinent to note that although *cut4* and *cut9* mutants have been shown to exhibit a high level of "*cut*" phenotype at the restrictive temperature, indicative of cell cycle defect (10, 12), our results showing enhanced chromosome loss, lagging chromosomes, and aberrant recombination are obtained at permissive temperature 25 °C. In light of the results shown above, we infer that the defects observed in *cut4* and *cut9* mutants at permissive temperature can be ascribed to the loss of heterochromatin (which can be correlated at molecular level with the lack of recruitment of Swi6, H3-Lys-9-Me2, and Clr4) and, thereby, of Cohesin to the centromeric and mating type heterochromatin.

We also analyzed the nuclear segregation phenotypes of APC mutants during meiosis. Examination of the four-spored asci by DAPI staining also revealed defective nuclear segregation during both the first and the second meiotic divisions in *sng2-1*, *cut4*, and *cut9* mutants. The effect was more at the second stage of meiosis II: 10–27% defective asci as compared with 2–8% asci having defective meiosis I. Thus, the aberration in heterochromatin structure in APC mutants may not only cause silencing defects but also exert deleterious effects on chromosomal integrity, inheritance, and segregation dynamics during mitosis and meiosis.

Lack of Cell Cycle Defect in APC Mutants at Permissive Temperature—Recently, it has been shown that the heterochromatin-bound fraction of Swi6 is reduced during G_2/M and elevated during S/late S phases (37). In this regard, it is formally possible that the length of M phase may be prolonged in APC mutants, although they are grown at permissive temperature during these studies. However, DAPI staining results showed no significant change in the fraction of cells in G_2/M among different APC mutants as compared with the wild type cells, thus ruling out that a prolonged G_2/M phase might contribute to the reduced localization of Swi6 in APC mutants.

Silencing Defect of APC Mutants Related to Reduced Ubiquitylation Activity—APC/C catalyzes the polyubiquitylation of Cdc13 and Cut2 (10, 12). It would be interesting to identify the target/mediator of APC in silencing. Indeed, degradation of Cohesin has been shown to be important for silencing in *S. cerevisiae* (38). To check whether the lack of degradation of a putative target like Cdc13, Cut2, Rad21, or any other hitherto unknown target, resulting from an inefficient ubiquitylation, might be responsible for the silencing defect, we studied the effect of overexpression of ubiquitin gene in *sng2-1*, *cut4-533*, and *cut9-665* mutants that exhibit silencing defect in the strain background *mat1Msmto REII*Δ *mat2*::*ura4*, as shown in Fig. 1, *B* and *D*. Interestingly, overexpression of His_6-tagged Ub strongly suppressed the silencing defect in all the mutants, as

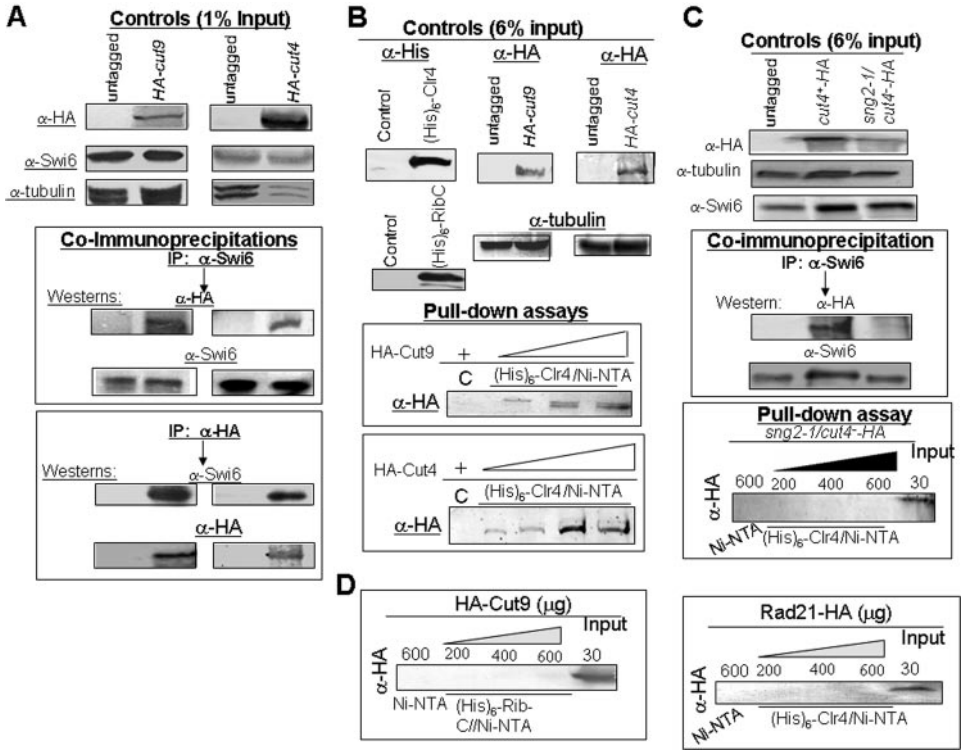

FIGURE 5. **Direct physical interaction of Cut4 and Cut9 with Swi6 and Clr4.** *A*, Cut4 and Cut9 interact with Swi6. Extracts from untagged strains and strains having HA-tagged copies of *cut4* and *cut9* genes were immunoprecipitated with anti-Swi6 (*upper panel*) or anti-HA antibody (*lower panel*) antibodies in the presence of EtBr (50 μg/ml) and subjected to SDS-PAGE followed by Western blotting with both antibodies (*lower panel*). *B*, Cut4 and Cut9 interact with Clr4 *in vitro*. A pull-down assay was performed by binding increasing concentrations of extracts from strains expressing HA-tagged Cut9 and Cut4 to Ni-NTA column on which His_6-tagged Clr4 was immobilized. The *C lane* represents Ni-NTA beads prebound with extracts from *E. coli* cells expressing the control vector alone followed by incubation with extracts from strain having HA-tagged *cut4* and *cut9* genes. The bound fractions were immunoblotted with anti-HA antibody. *C*, mutant HA-tagged Cut4 protein does not interact with Swi6 and Clr4 *in vitro*. Co-immunoprecipitation was performed using extracts from untagged WT strain and WT and *sng2-1/cut4*$^-$ mutant strains having the *cut4* gene tagged with HA at the N terminus. The extracts were immunoprecipitated with anti-Swi6 antibody and immunoblotted with both anti-Swi6 and anti-HA antibodies. A pull-down assay was carried out by incubating extracts from WT and *sng2-1/cut4*$^-$ mutant, having the chromosomally tagged *cut4* gene, at increasing concentrations with Ni-NTA resin on which His_6-Clr4 was immobilized. The blot probed with anti-HA antibody is shown in the *lower panel*. The *C lane* represents beads prebound with extract from *E. coli* cells expressing the control vector alone followed by incubation with the wild type HA-Cut4 extract. The *Input lane* contains the extract from the mutant strain with HA tagged *sng2-1/cut4*$^-$ mutant gene. *D*, lack of binding of HA-tagged Cut9 and Rad21 to RibC and Clr4, respectively, *in vitro*. Extracts prepared from a strain expressing HA-tagged Cut9 were incubated at increasing concentrations with Ni-NTA beads to which extract from *E. coli* cells expressing His_6-RibC was bound (*left panel*). Similarly, extract from *S. pombe* cells expressing HA-tagged *rad21* gene was incubated with Ni-NTA beads to which extract from *E. coli* cells expressing His_6-tagged Clr4 was bound (*right panel*). The *C lane* represents the control lane where beads alone were used. The *Input lanes* show the extracts from cells expressing HA-Cut9 (*left panel*) and HA-Rad21 (*right panel*). After SDS-PAGE, gels were immunoblotted with anti-HA antibody. The samples of HA-Rad21 were subjected to a shorter electrophoresis run and, therefore, did not resolve the multiple phosphorylated bands.

measured by the number of iodine-staining colonies (Fig. 7, *A* and *B*), the level of haploid meiosis (not shown), suppression of the level of *ura4* transcript (Fig. 7*C*), and the lagging chromosome phenotype of *cut4-533* and *cut9-665* mutants (Fig. *7D*). More importantly, His-Ub partially restored the level of Swi6 at mating type in both *cut4*$^-$ and *cut9*$^-$ mutants, although no effect was observed on the level of Myc-tagged Clr4 and H3-Lys-9-me2 (data not shown). No deleterious effect of expression of His-Ub vector on cell viability was observed. Thus, the silencing defect in APC mutants may be caused by their reduced catalytic ubiquitylation efficiency.

Bidirectional Transcription from dh Repeats in APC Mutants—Recently, mutations in cullin subunit *cul4* have been shown to cause similar defects in silencing and, in addition, also shown to elicit bidirectional expression of transcription from the *dh* repeats (39), similar to that observed in the case of RNAi as well as *clr4*Δ mutants (6). We checked whether the APC subunits may also play a similar role. Interestingly, as in the case of *clr4*Δ and *dcr1*Δ strains, mutants *sng2-1*, *cut4-533*, and *cut9-665* all exhibit bidirectional transcription (Fig. 8). As shown earlier (6), *swi6*Δ strain showed no such effect (Fig. 8).

DISCUSSION

It is thought that heterochromatin assembly is initiated by the RNAi pathway via an initial establishment of the H3-Lys-9 dimethylation mark, which is then bound by the chromodomain protein Swi6/HP1. Subsequently, multimerization of Swi6 together with an interaction with the histone methyltransferase Clr4 helps in spreading the heterochromatin. (Alternative pathways exist where Atf1-mediated recruitment of Clr4 occurs independently of RNAi (29, 40).) Swi6, in turn, recruits the Cohesin complex, which is important for sister chromatid cohesion and for imparting greater chromatin integrity to the mating type region.

Parallel work in the area of cell cycle control has shown that APC-E3 ligase ubiquitylates cyclin Cdc13, which is then degraded by the proteasome pathway, triggering the exit of the cells from mitosis. In addition, APC also ubiquitylates Securin/Cut2, whose degradation by proteasome releases the Separase/Cut1. Cut1, in turn, degrades the Rad21 subunit of the Cohesin complex, thus allowing sister chromatid separation during metaphase-to-anaphase transition. Thus, the main function of APC is believed to be during mitosis in ensuring sister chromatid separation and mitotic exit.

APC and Swi6/Clr4 Cooperate to Establish Silencing—The present study shows an additional, surprising role of APC, as indicated by the following observations. (i) APC mutants exhibit silencing defects at mating type, centromere, and rDNA loci; (ii) APC is required for recruitment of Swi6, H3-Lys-9-Me2, and Clr4 to heterochromatin loci. (iii) Swi6, in turn, is necessary for recruitment of APC subunits Cut4 and Cut9 to heterochromatin. (iv) The mutual recruitment is mediated by

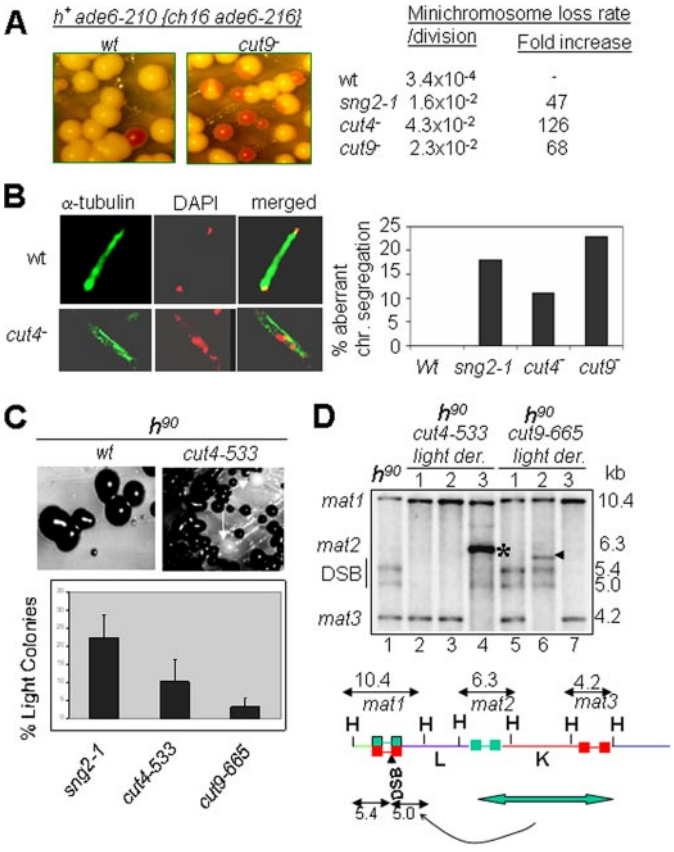

FIGURE 6. **Mutations in APC subunits affect chromosomal segregation and integrity.** *A*, elevated rate of chromosomal loss in *sng2-1*, *cut4-533*, and *cut9-665* mutants. Wild type strains having a resident *ade6-210* allele and an artificial chromosome Ch16 harboring an *ade6-210* allele appear *white* on adenine-limiting plates (YE (15, 16)) because of interallelic complementation. The loss of the extra chromosome unmasks the red colony phenotype due to the *ade6-210* allele. The chromosomal loss rate was determined (17) and found to be greatly elevated in the mutants as compared with the wild type strains. *B*, lagging chromosome phenotype in APC mutants. Dividing cells of wild type and mutant strains were stained with DAPI for nuclear staining and with anti-α-tubulin antibody and visualized by confocal microscopy. At least 300 cells were counted. *C* and *D*, elevated level of aberrant recombination in the mating type region in APC mutants. Upon restreaking, cells from colonies of *cut4-533* and *cut9-665* mutant strains in the switching, homothallic background (h^{90}), which give dark staining with iodine, produce colonies that give light staining with iodine (indicated by *arrows*) at an elevated rate. The histogram shows the quantitation of the light-staining colonies. *D*, Southern blot analysis of the HindIII digests of DNA from light-staining colonies show rearrangements in the mating type region, including lack of double strand break (*lanes 2* and *3* in *cut4-533* mutant and *lane 7* in *cut9-665* mutant) and other rearrangements, like deletion of *mat3* locus (indicated by * in *cut4-533* mutant (*lane 4*) and *arrowhead* in *cut9-665* mutant (*lane 6*)). The *lower panel* shows the schematic representation of the mating type region, indicating the HindIII fragments representing the cassettes *mat1*, *mat2*, and *mat3* with sizes of 10.4, 6.3, and 4.2 kb, respectively (35). The formation of DSB at *mat1* generates additional fragments of 5.4 and 5.0 kb. Duplicative transposition of the entire *mat2-mat3* interval onto the *mat1* locus yields the h^+ rearrangement. HindIII digests of the DNA from the indicated strains were resolved by 0.8% agarose gel electrophoresis, Southern blotted, and hybridized with the 10.4-kb mat1M HindIII probe radiolabeled with [α-^{32}P]dCTP followed by autoradiography, as described (36, 41). Because of the lower extent of homology with the mat1M probe, the *mat2P* signal at 6.3 kb is very faint.

direct physical interaction of Cut4 and Cut9 with Swi6 and Clr4. (v) APC mutants are also defective in Cohesin/Rad21 recruitment at the centromere, possibly as an indirect consequence of the loss of Swi6 recruitment, which is known to be required for Cohesin recruitment. Other defects including lagging chromosomes, chromosomal rearrangements, enhanced chromosome loss during mitosis, and defective chromosome segregation during meiosis I and II may be ascribed to the loss of heterochromatin stability at the centromere and mating type because of depletion of Swi6, Clr4, and Cohesin.

It remains to be determined as to which event occurs first, recruitment of APC or that of Swi6, which, once initiated, sets up a positive reinforcing loop of mutual recruitment of Swi6/Clr4 and APC. In this regard, earlier work from our laboratory has shown that recruitment of Swi6/HP1 is coupled to DNA replication by virtue of direct physical interaction of polα with Swi6 (13, 14). It has further been shown in both *S. cerevisiae* and *S. pombe* that Cohesin is recruited during DNA replication (11). Thus, it remains to be seen whether the APC complex may also be recruited to heterochromatin regions during DNA replication. In this regard, it is interesting to note that *polα* can suppress the ts phenotype of the *sng2-1*/*cut4*$^-$ and *cut4-533* mutants. However, *polα* does not suppress the silencing defect of *cut4-533* and *sng2-1* mutants (data not shown), suggesting that some other mechanism may also operate. Interestingly, preliminary results show that although overexpression of Swi6 can suppress the level of expression of *ura4* reporter located at *otr1R* region in *cut9-665* mutant, *cut9* gene does not repress the expression of *ura4* in *swi6* mutant (data not shown). These results suggest that Swi6 may act downstream of APC. Further experiments will analyze the chain of events at molecular level.

Role of Multiple Ubiquitylation Pathway in Silencing—Rad6 and Rhp6, the E2-ubiquitin-conjugating (E2) ubiquitin-conjugating enzymes, have been shown to play a role in silencing in *S. cerevisiae* and *S. pombe*, respectively (41–43). In *S. cerevisiae*, RAD6-dependent monoubiquitination at the Lys-123 position in histone H2B (44) elicits histone H3 methylation at Lys-4 in a trans-regulatory pathway (45). In *S. pombe*, Rhp6 is also required for H3-Lys-4-dimethylation and monoubiquitination of histone H2B (46).[6] However, unlike in *S. cerevisiae*, H3-Lys-4 methylation is associated with euchromatic regions in *S. pombe*. Thus, there may be another target of action for Rhp6 that may be responsible for silencing in *S. pombe*. A histone-interacting protein Uhp1 has been identified in *S. pombe* as a candidate target or mediator of Rhp6 in silencing (47).

Recent reports have indicated a role of Cul4 subunit of cullin E3 ligase in recruitment of Clr4 to heterochromatin. Cul4 has been shown to associate with Rik1 (39, 48, 49), Raf1, Raf2, Pip1, and H2B (48). Although *cul4*Δ mutation causes reduction of H3-Lys-9 dimethylation and Swi6 binding (48), deletion of *raf1* and *raf2* resulted in increased H3-Lys-4-Me2 level and decrease in the H3-Lys-9-Me2 level at the centromeric heterochromatin (49). Our results with APC are similar to those of Horn *et al.* (48) as the mutants *sng2-1*, *cut4-533*, *cut9-665*, and *nuc2* show reduced Swi6 and H3-Lys-9-Me2 at centromeric *dh* repeats (Fig. 3) as well as an increase in H3-Lys-4-Me2 (data not shown). Significantly, the silencing defect in both *cul4* and *sng2-1* mutants can be related to reduced efficiency or limitation of ubiquitylation activity (Ref. 48 and the present study). Because E3 ligase functions in recognition of specific targets for ubiquitylation, the targets, through which APC and cullin sub-

[6] A. Saini and J. Singh, unpublished results.

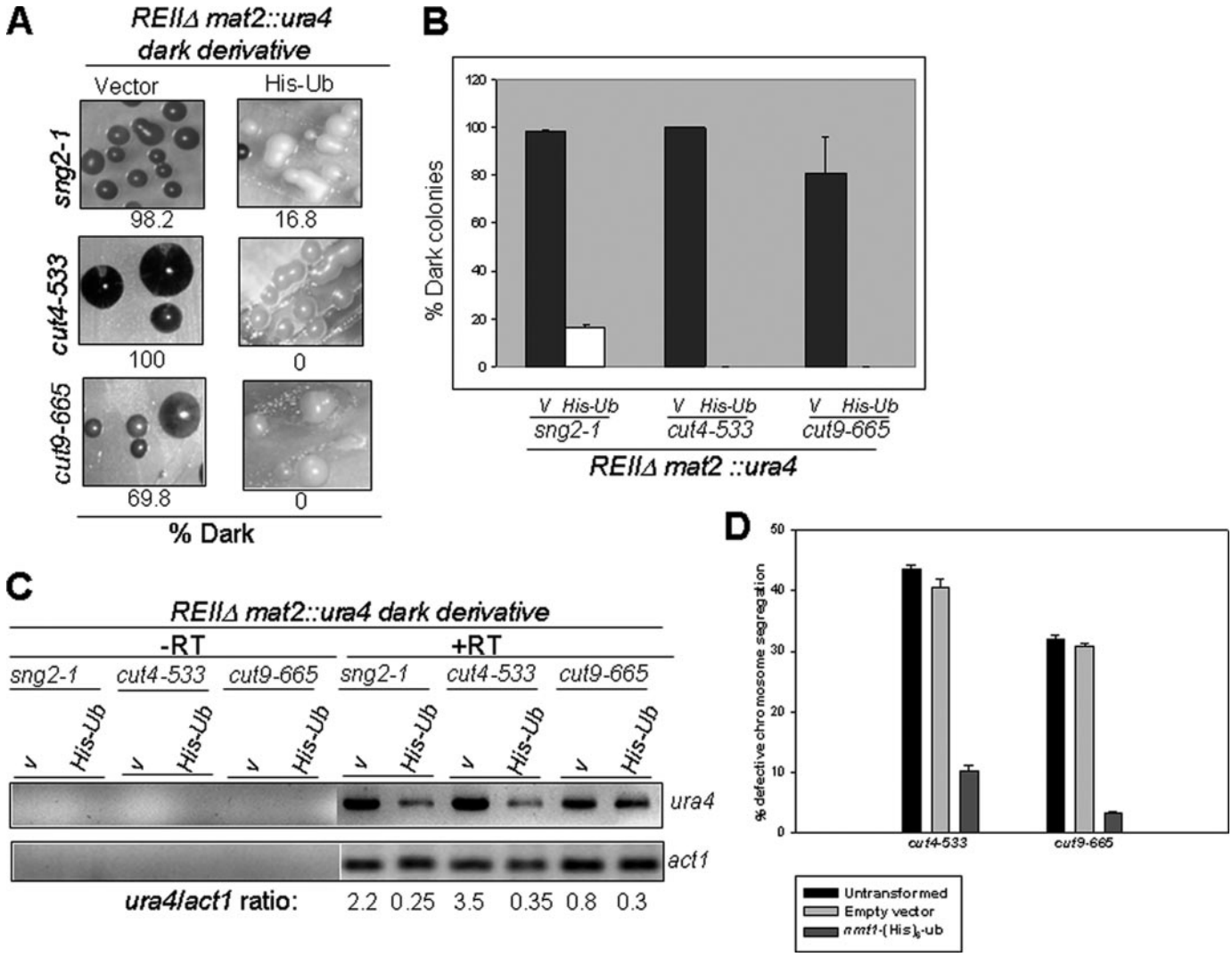

FIGURE 7. **Suppression of silencing defect in APC mutants by overexpression of Ubiquitin.** *A–C*, dark-staining colonies of *sng2-1*, *cut4-533*, and *cut9-665* mutants in the genetic background *Msmto REIIΔmat2::ura4* were transformed with the control vector pREP3 (*V*) and vector expressing His-Ub under the control of *nmt1* promoter. *A*, transformants were grown on selective sporulation plates in absence of thiamine, and the colonies were subjected to iodine staining. *B*, the percentage of dark colonies representing the repressed state were plotted from the average of five measurements as a histogram. At least 200 colonies were counted for each measurement. *C*, transcripts for the *mat2P*-linked *ura4* and *act1* were amplified by RT-PCR and visualized following agarose gel electrophoresis by staining with EtBr. *V* stands for empty vector PREP3. *D*, overexpression of His-Ub suppresses the lagging chromosome phenotype of *cut4-533* and *cut9-665* mutants. Mutant strains harboring the empty vector and His_6-Ub under the control of *nmt1* prompter were grown in PMA medium lacking thiamine. The lagging chromosome phenotype was monitored by staining cells with DAPI after culturing initially at 25 °C and then shifting to 18 °C for 8–10 h. 300 cells were counted in triplicate for each measurement.

unit Cul4 function, may be different. Thus, it is possible that multiple ubiquitylated targets may play a role in silencing.

The putative targets/mediators of APC may include Rad21, although there could be more than one target, like Swi6, Clr4, Chp1, or a hitherto unknown target. Significantly, degradation of Rad21 has been shown to be important for mating type silencing in *S. cerevisiae* (38). Recently, sumoylation of Swi6, Clr4, and Chp1 has been shown to be critical for stable silencing (50). It remains to be investigated whether APC regulates the ubiquitylation of Swi6 or Clr4. Our preliminary results do indicate that Swi6 undergoes efficient monoubiquitylation in wild type strain but at a much lower level in the *cut4* and *cut9* mutants. Further studies will attempt to investigate whether Swi6 or any other target indeed acts as the target/mediator of APC and has a role in silencing.

Recently, Hsk1-Dfp1-mediated phosphorylation of Swi6 has been shown to be critical for stabilizing the binding of Swi6 to heterochromatin (7). Phosphorylation causes a reduction in the electrophoretic mobility of Swi6 (7). However, no change in either the level or the electrophoretic mobility of Swi6 was observed in APC mutants as compared with wild type, indicating that APC does not regulate the phosphorylation of Swi6 (data not shown).

A Possible Role of APC in RNAi Pathway—A rather surprising finding in this study is that, as shown in the case of *cul4* mutant, the APC mutants show bidirectional transcription from the *dh* repeats (39). It has been proposed that Rik1-Cul4-E3 ligase complex may recruit Clr4 and cause H3-Lys-9 dimethylation (48, 49, 51). Thus, both Cullin and APC-E3 ligase pathways may provide alternate routes by which H3-Lys-9 dimethylation can be estab-

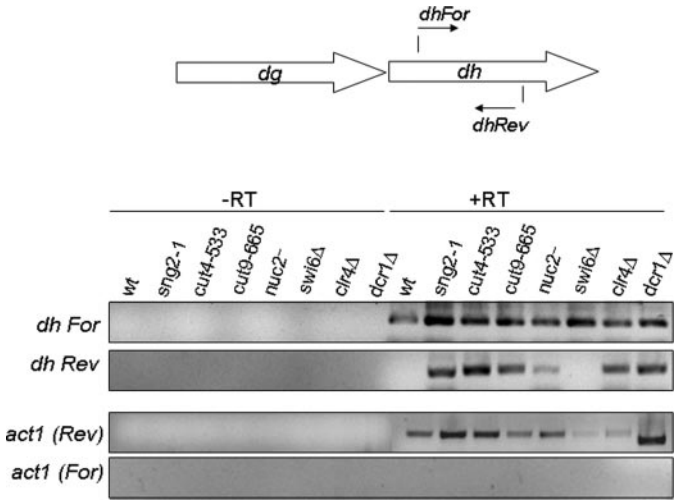

FIGURE 8. **Bidirectional transcription from both the strands of the *dh* repeat region in APC mutants.** RNA prepared from WT, *sng2-1*, *cut4-533*, *cut9-665*, *nuc2*, *swi6*Δ, *clr4*Δ, and *dcr1*Δ strains was subjected to RT-PCR analysis. The cDNA synthesis step was carried out using the forward (*For*) and reverse (*Rev*) primers for *dh* and *act1* in the absence (−*RT*) or presence (+*RT*) of MuLV reverse transcriptase followed by PCR. The products were visualized by staining with EtBr after they were resolved by agarose gel electrophoresis.

lished. The possible interaction of APC with the components of the RNAi pathway remains to be investigated further.

The main novel finding of this study is that the assembly of heterochromatin occurs through cooperative interaction of APC subunits with Swi6 and Clr4. This interaction is critical for both silencing and stable heterochromatin organization and inheritance. It is tempting to speculate that coordination between Swi6-mediated recruitment of APC and that of the Cohesin complex may not only stabilize silencing and heterochromatin but may also have an impact on the subsequent events of Cohesin degradation and sister chromatid separation, as depicted in the speculative model. These intriguing possibilities remain to be tested. Interestingly, Tsg24, a murine homolog of Cut4/Apc1, has also been shown to be associated with centromere and play a role in sister chromatid separation (52). Another homolog bimE in *Aspergillus nidulans* functions as a mitotic check point regulator (53). As APC/C, Cohesin, and heterochromatin components, like Swi6/HP1, are highly conserved during evolution, the role of APC/C in recruitment of Swi6/HP1 and Clr4/Suv39 in heterochromatin assembly may also be evolutionarily conserved.

Acknowledgments—We are grateful to A. Klar for strains, M. Yanagida for the gift of the cut4-533 mutant, the vector pREP41N-HAcut4, the cut4 gene in integrating vector pYY439, and a high copy vector pYY463, Robin Allshire for strain FY2002 and the strain having Ch16 chromosome, K. Ekwall for the strain HU393, A. Pidoux for the plasmid expressing green fluorescent protein-tagged Swi6 under the control of nmt1 promoter vector, G. Thon for the strain PG1649, J.-P. Javerzat for the HA-Rad21 tagged strain, S. Moreno for the His-Ub vector, K. Gould for cut9-665 and nuc2 mutants and the strain having the HA-tagged cut9 gene, A. Kumar for the mis6 and swi6 mutant strains in the cnt1::ura4 and imr1::ura4 genetic backgrounds, respectively, and S. Karthikeyan for the purified protein His$_6$-RibC.

REFERENCES

1. Wang, G., Ma, A., Chow, C. M., Horsley, D., Brown, N. R., Cowell, I. G., and Singh, P. B. (2000) *Mol. Cell Biol.* **20,** 6970–6983
2. Grewal, S. I., and Elgin, S. C. (2002) *Curr. Opin. Genet. Dev.* **12,** 178–187
3. Bannister, A. J., Zegerman, P., Partridge, J. F., Miska, E. A., Thomas, J. O., Allshire, R. C., and Kouzarides, T. (2001) *Nature* **410,** 120–124
4. Hall, I. M., Shankaranarayana, G. D., Noma, K., Ayoub, N., Cohen, A., and Grewal, S. I. (2002) *Science* **297,** 2232–2237
5. Noma, K., and Grewal, S. I. (2002) *Proc. Natl. Acad. Sci. U. S. A.* **99,** 16438–16445
6. Volpe, T. A., Kidner, C., Hall, I. M., Teng, G., Grewal, S. I., and Martienssen, R. A. (2002) *Science* **297,** 1833–1837
7. Bailis, J. M., Bernard, P., Antonelli, R., Allshire, R. C., and Forsburg, S. L. (2003) *Nat. Cell Biol.* **5,** 1111–1116
8. Bernard, P., Maure, J. F., Partridge, J. F., Genier, S., Javerzat, J. P., and Allshire, R. C. (2001) *Science* **294,** 2539–2542
9. Nonaka, N., Kitajima, T., Yokobayashi, S., Xiao, G., Yamamoto, M., Grewal, S. I., and Watanabe, Y. (2002) *Nat. Cell Biol.* ***4*** **1,** 89–93
10. Yanagida, M., Yamashita, Y. M., Tatebe, H., Ishii, K., Kumada, K., and Nakaseko, Y. (1999) *Philos. Trans. R. Soc. Lond. B Biol. Sci.* **354,** 1559–1569
11. Uhlmann, F. (2004) *Exp. Cell Res.* **296,** 80–85
12. Yamashita, Y. M., Nakaseko, Y., Samejima, I., Kumada, K., Yamada, H., Michaelson, D., and Yanagida, M. (1996) *Nature* **384,** 276–279
13. Ahmed, S., Saini, S., Arora, S., and Singh, J. (2001) *J. Biol. Chem.* **276,** 47814–47821
14. Nakayama, J., Allshire, R. C., Klar, A. J., and Grewal, S. I. (2001) *EMBO J.* **20,** 2857–2866
15. Moreno, S., Klar, A., and Nurse, P. (1991) *Methods Enzymol.* **194,** 795–823
16. Allshire, R. C., Nimmo, E. R., Ekwall, K., Javerzat, J. P., and Cranston, G. (1995) *Genes Dev.* **92,** 218–233
17. Kipling, D., and Kearsey, S. E. (1990) *Mol. Cell Biol.* **10,** 265–272
18. Lorentz, A., Ostermann, K., Fleck, O., and Schmidt, H. (1994) *Gene* (*Amst.*) **143,** 139–143
19. Bahler, J., Wu, J. Q., Longtine, M. S., Shah, N. G., McKenzie, A., III, Steever, A. B., Wach, A., Philippsen, P., and Pringle, J. R. (1998) *Yeast* **14,** 943–951
20. Ekwall, K., and Partridge, J.F. (1999) in *Chromosome Structural Analysis: A Practical Approach* (Bickmore W. A., ed) pp. 38–57, Oxford University Press, Oxford, UK
21. Lai, J.-S., and Herr, W. (1992) *Proc. Natl. Acad. Sci. U. S. A.* **89,** 6958–6962
22. Grewal, S. I., and Klar, A. J. (1996) *Cell* **86,** 95–101
23. Thon, G., and Friis, T. (1997) *Genetics* **145,** 685–696
24. Thon, G., Bjerling, K. P., and Nielsen, I. S. (1999) *Genetics* **151,** 945–963
25. Yoon, H. J., Feoktisova, A., Wolfe, B. A., Jennings, J. L., Link, A. J., and Gould, K. L. (2002) *Curr. Biol.* **12,** 2048–2054
26. Tomonaga, T., Nagao, K., Kawasaki, Y., Furuya, K., Murakami, A., Morishita, J., Yuasa, T., Sutani, T., Kearsey, S. E., Uhlmann, F., Nasmyth, K., and Yanagida, M. (2000) *Genes Dev.* **14,** 2757–2770
27. Grewal, S. I., and Klar, A. J. (1997) *Genetics* **146,** 1221–1238
28. Sadaie, M., Iida, T., Urano, T., and Nakayama, J. (2004) *EMBO J.* **23,** 3825–3835
29. Kim, H. S., Choi, E. S., Shin, J. A., Jang, Y. K., and Park, S. D. (2004) *J. Biol. Chem.* **279,** 42850–42859
30. Kumada, K., Su, S., Yanagida, M., and Toda, T. (1995) *J. Cell Sci.* **108,** 895–905
31. Pidoux, A. L., Uzawa, S., Perry, P. E., Cande, W. Z., and Allshire, R. C. (2000) *J. Cell Sci.* **113,** 4177–4191
32. Ekwall, K., Javerzat, J. P., Lorentz, A., Schmidt, H., Cranston, G., and Allshire, R. (1995) *Science* **269,** 1429–1431
33. Ekwall, K., Nimmo, E. R., Javerzat, J. P., Borgstrom, B., Egel, R., Cranston, G., and Allshire, R. (1996) *J. Cell Sci.* **109,** 2637–2648
34. Beach, D. H., and Klar, A. J. (1984) *EMBO J.* **3,** 603–610
35. Egel, R., Beach, D. H., and Klar, A. J. (1984) *Proc. Natl. Acad. Sci. U. S. A.* **81,** 3481–3485
36. Singh, J., and Klar, A. J. (1993) *Nature* **361,** 271–273

37. Chen, E. S., Zhang, K., Nicolas, E., Cam, H. P., Zofall, M., and Grewal, S. I. (2008) *Nature* **451,** 734–737
38. Lau, A., Blitzblau, H., and Bell, S. P. (2002) *Genes Dev.* **16,** 2935–2945
39. Thon, G., Hansen, K. R., Altes, S. P., Sidhu, D., Singh, G., Verhein-Hansen, J., Bonaduce, M. J., and Klar, A. J. (2005) *Genetics* **171,** 1583–1595
40. Jia, S., Noma, K., and Grewal, S. I. (2004) *Science* **304,** 1971–1976
41. Singh, J., Goel, V., and Klar, A. J. (1998) *Mol. Cell Biol.* **18,** 5511–5522
42. Huang, H., Kahana, A., Gottschling, D. E., Prakash, L., and Liebman, S. W. (1997) *Mol. Cell Biol.* **17,** 6693–6699
43. Nielsen, I. S., Nielsen, O., Murray, J. M., and Thon, G. (2002) *Eukaryot. Cell* **1,** 613–625
44. Robzyk, K., Recht, J., and Osley, M. A. (2000) *Science* **287,** 501–504
45. Sun, Z. W., and Allis, C. D. (2002) *Nature* **418,** 104–108
46. Roguev, A., Schaft, D., Shevchenko, A., Aasland, R., Shevchenko, A., and Stewart, A. F. (2003) *J. Biol. Chem.* **278,** 8487–8493
47. Naresh, A., Saini, S., and Singh, J. (2003) *J. Biol. Chem.* **278,** 9185–9194
48. Horn, P. J., Bastie, J. N., and Peterson, C. L. (2005) *Genes Dev.* **19,** 1705–1714
49. Jia, S., Kobayashi, R., and Grewal, S. I. (2005) *Nat. Cell Biol.* **7,** 1007–1013
50. Shin, J. A., Choi, E. S., Kim, H. S., Ho, J. C., Watts, F. Z., Park, S. D., and Jang, Y. K. (2005) *Mol. Cell* **19,** 817–828
51. Horn, P. J., and Peterson, C. L. (2006) *Chromosome Res.* **14,** 83–94
52. Jorgensen, P. M., Brundell, E., Starborg, M., and Hoog, C. (1998) *Mol. Cell Biol.* **18,** 468–476
53. James, S. W., Mirabito, P. M., Scacheri, P. C., and Morris, N. R. (1995) *J. Cell Sci.* **108,** 3485–3499